IHJPAS. 36(2)2023

Ibn Al-Haitham Journal for Pure and Applied Sciences
Journal homepage: jih.uobaghdad.edu.iq

Synthesis a Novel Complexes of VO(II),Mn(II),Fe(II) ,Co(II), Ni(II), Cu(II)and Pt(IV) Derived from Schiff's Base of Pyridoxal and 2-amino-4-nitrophenol and Study their Biological Activates

Ahmed A. Ismail
Department of Chemistry, College of Education for Pure Science Ibn Al-Haitham, University of Baghdad, Baghdad, Iraq.
chem3ps@gmail.com

Sajid M. Lateef
Department of Chemistry, College of Education for Pure Science, University of Diyala, Diyala, Iraq.
sajidm1957@gmail.com

Article history: Received 1 October 2022, Accepted 24 October 2022, Published in April 2023.

doi.org/10.30526/36.2.3054

Abstract

This work describes the synthesis of novel ligand (H_2L^2) (4-((2-hydroxy-5-nitrophenyl)imino)methyl)-5(hydroxymethyl)-2methylpyridin-3-ol) type (NOO) donor atoms. When it coordinates with metal ions[V^{2+},Mn^{2+},Fe^{2+},Co^{2+},Ni^{2+},$Cu^{2+}$and Pt^{4+}] with the general formula $K_2[M(L^2)_2].XH_2O$ and $K_2[VO(L^2)(OSO_3)].H_2O$. This ligand can form tridentate structures. The ligand was synthesized from the reaction of pyridoxal hydrochloride with 2-amino-4-nitrophenol in ethanol (as a solvent) at a mole ratio of 1:1 and thoroughly mixed and refluxed for 6-8 hrs . The reaction was monitored using TLC (Ethylactate/hexane 1:1). The structures of the ligand and the complexes were characterised using spectroscopic techniques such as (FT-IR, ^{1}HNMR, ^{13}CNMR, UV-Vis, and Mass spectroscopy). In addition, molar conductance, magnetic susceptibility, elemental analysis, and thermo gravimetric, melting points were also measured for complexes. The antibacterial activities of the obtained products were tested against G- bacteria (*Klebsiella pneumoniae and pseudomonas*), G+ bacteria (*Staphylococcus aureus and Bacillus subtilis*). In addition, antifungal action was tested against (*Candida albicans*). The results were good in both tests.

keywords: donor atoms, ligand**,** pyridoxal hydrochloride**.**

1. Introduction

Heterocyclic compounds are a part of organic compounds in which it is contain hetero atoms in addition to carbon in their aromatic ring, the atoms could be nitrogen, sulfur and oxygen [1]. There are numerous heterocyclic compounds that may be synthesized in the laboratory and may have significant properties as variables[2]. Heterocyclic compounds are a big group of organic chemicals because of their biological properties such as anti-bacterial, anti-fungal, anti-inflammatory, and anti-cancer properties. [3] The use of nitrogen-containing heterocycles compounds are in medicine, industry, and agriculture attracts attention of the many researchers [4]. Schiff base that derived from pyridoxal consist an important class of heterocyclic compounds and being the core structure in several natural product and which have biological applications [5]. The nitro phenol compounds were utilized in the reactions as intermediates especially in the pharmaceuticals, pesticides, dyes and wood preservation. Environmental degradation of 2,4-dinitrophenol lead to form *o*-amino-*p*-nitrophenol which can be used as a fungicide for wood [6]. Schiff's base complexes contains a variety of central metal atoms, including Cu, Ni, Co, and Pt, have been extensively reported for their diverse crystallographic properties, enzymatic reactions, mesogenic properties, catalystic and magnetic properties, as well as their critical role in the interpreting the transition metal coordination in chemistry[7].

2. Materials and method

Several different methods and devices were used to characterize the targeted compounds. These are Melting Point, FT-IR spectrophotometry, Conductivity, UV.Vis photometer in the area of (400-1100) nm, Mass spectrophotometry, Metal Analysis, Elemental analysis, Magnetic Moment Measurement, ^{1}H and ^{13}C-NMR photometer and Thermal Gravimetric Analysis TGA. The biological activity of the prepared compounds was then evaluated towards (*Klebsiella pneumoniae and pseudomonas*) (G-), two bacteria (*Staphylococcus aureus and Bacillus subtilis*) (G+), and one fungus (*Candida albicans*).

2.1. Synthesis of ligand H_2L^2:

The solution of pyridoxal hydrochloride (2.03g, 0.01mol) in ethanol was added to the solution of 2-amino-4-nitrophenol (0.151g, 0.01mol) in the same solvent at a mole ratio of 1:1 and thoroughly mixed. To correct the pH (pH = 7-8), catalytic 0.1% alcoholic NaOH was added to the reaction mixture, and the reaction was heated under reflux for 6–8 hour [8]. The TLC silica gel was used for monitored the reaction eluent (1:1 Ethylactate/hexane). A solid mass of dark brown hue that formed during reflux and was cooled to room temperature and then, washed with

ethanol to give 86% yield as reddish brown, m.p:100-102 ºC , Mw:303.27 $C_{14}H_{13}N_3O_5$, Synthesis route of the ligand [H_2L^2] shown in Equation (1).

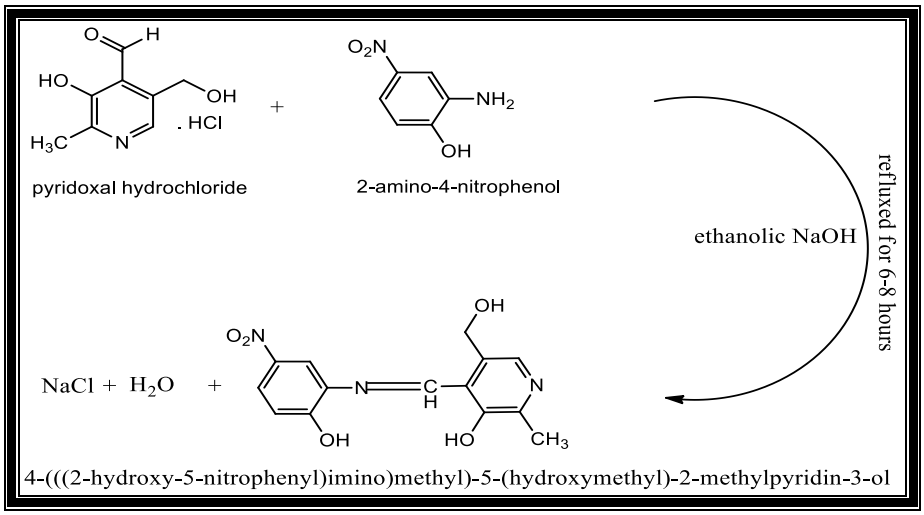

Equation (1): synthesis route of the ligand [H_2L^2].

2.2. FT-IR spectra of starting materials and the ligand H_2L^2

2.2.1. Analysis of FT-IR spectra:

2.2.1.1. Spectrum of Pyridoxal:

Figure (S1) shows band at 3259 cm^{-1} belongs to O-H group, bands at 3047 cm^{-1} for C-H aromatic and at 2978 cm^{-1} due to C-H aliphatic. The band at 1643 cm^{-1} refers to C=O, the strong band at 1554 cm^{-1} belong to the frequency of C=N in the ring and the band at 1442 cm^{-1} is for aromatic C=C. The two bands at 1284 and 783 cm^{-1} refers to C-O and C-O that exist in the compound [9]. see table 1.

2.2.1.2. FT-IR spectrum of 2-amino-4-nitrophenol (ANPH):

Two sharps bands appeared at 3471 and 3387 cm^{-1} for NH_2 group, and the band at 1635 cm^{-1} and a strong band at 1581 refers to N-H bending and C=N respectively [10], aromatic C=C appeared at 1523 cm^{-1}. Moreover, band of C-N is located at 1338 cm^{-1}. The two bands at 1292 and 779 cm^{-1} assigned for two C-O [11]. see table 1.

2.2.1.3. FT-IR spectrum for ligand H_2L^2:

The spectrum of (H_2L^2) showed in figure (S1), band at 3356 cm^{-1} is for O-H group. The C-H aromatic appeared at 3070 cm^{-1}. The stretching frequency of the imine group υ(C=N) appeared at 1620 cm^{-1} and band at 1581 cm^{-1} belong to C=N within the group [12]. The aromatic C=C appeared at 1496 cm^{-1} and band at 1334 cm^{-1} assigned for C-N. The bands at 1288 and 744 cm^{-1} refers to both C-O. see table 1.

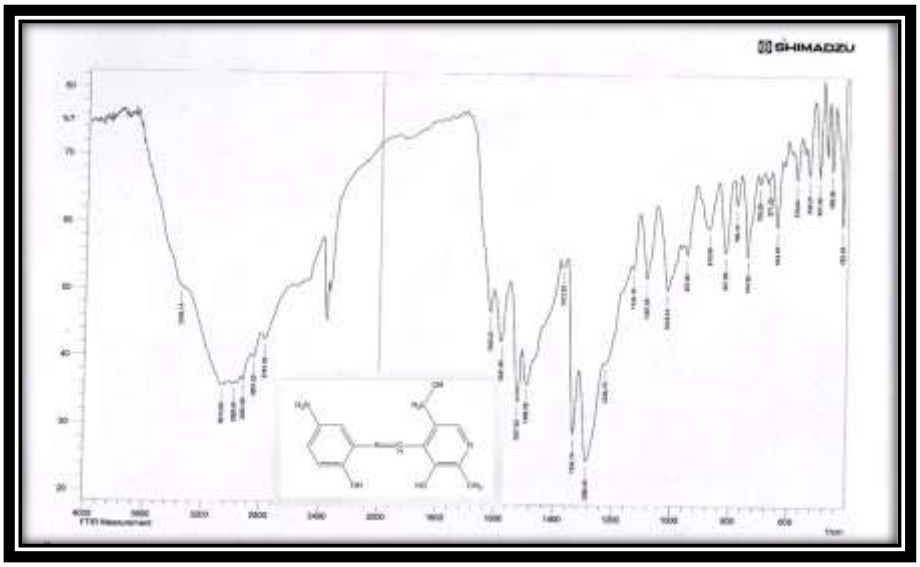

Figure(S1): FT-IR spectrum of the H_2L^2

Table (1): Infra-red data (cm^{-1}) for the starting materials and the ligand

Compounds	υ(O-H)	υasy(NH_2) υsy(NH_2)	υ(C=O)	υ(C-H) aro. υ(C-H) ali.	υ(C=N) imine	υ(C=N) in plane	υ(C-N)	υ(C - O) δ(C - O)
Pyridoxal	3259	-	1643	3047 2978	-	1554	-	1284 783
ANPH	-	3471 3387	-	3047 2997	-	1581	1338	1292 779
H_2L^2	3356	- -	-	3070 2985	1620	1581	1334	1288 744

2.3. The Mass spectra of H_2L^2:

The molecular ion peak for the ligand is observed at m/z^+ =303$[M]^{\cdot}$ =$C_{14}H_{13}N_3O_5$; requires = 303.09[13]. The peaks detected at m/z^+ = 285 correspond to $[C_{14}H_{11}N_3O_4]^{\dot{+}}$ - $[H_2O]$ The fragmentation pattern of (H_2L^2) is tabulated in Table (2). See scheme 1 for proposed fragmentation of (H_2L^2).

Table (2): The fragments pattern of [H_2L^2]

H_2L^2			
FRAGMENTS	**FORMULA**	**Mwt**	**Abundance**
$[M]^{\cdot}$	$C_{14}H_{13}N_3O_5$	303	2109597.6
$[M_1]^{\dot{+}}$ = $[M]^{\cdot}$- H_2O	$C_{14}H_{11}N_3O_4$	285	82038.9
$[M_2]^{\dot{+}}$ = $[M_1]^{\dot{+}}$ - O	$C_{14}H_{11}N_3O_3$	269	16579.8
$[M_3]^+$ = $[M_2]^{\dot{+}}$ - CH	$C_{13}H_{10}N_3O_3$	256	40586.4
$[M_4]^{\dot{+}}$ = $[M_3]^+$- C_5H_2N	$C_8H_8N_2O_3$	180	271210.2
$[M_5]^{\dot{+}}$ = $[M_4]^{\dot{+}}$ - NH	$C_8H_7NO_3$	165	661036.3

$[M_6]^{\dot{+}} = [M_5]^{\dot{+}} - C$	$C_7H_7NO_3$	153	1398016
$[M_7]^+ = [M_6]^{\dot{+}} - CH_3$	$C_6H_4\ NO_3$	138	644713.6
$[M_8]^{\dot{+}} = [M_7]^+ - N$	$C_6H_4\ O_3$	124	821425.8
$[M_9]^{\dot{+}} = [M_8]^+ - O$	$C_6H_4\ O_2$	108	4600451.6
$[M_{10}]^{\dot{+}} = [M_9]^{\dot{+}} - C$	$C_5H_4\ O_2$	96	1913392.6
$[M_{11}]^{\dot{+}} = [M_{10}]^{\dot{+}} - O$	C_5H_4O	80	3456116.7
$[M_{12}]^+ = [M_{11}]^{\dot{+}} - OH$	C_5H_3	63	2108557.6
$[M_{13}]^+ = [M_{12}]^+ - C$	C_4H_3	51	4095603

2.4. ^{1}H-NMR spectrum for the ligand H_2L^2

^{1}H-NMR spectrum for (H_2L^2) displayed the peaks at 7.22–6.79 ppm as multiple are assignable to aromatic ring protons (Ar–CH)[14] . The signal at 8.19 ppm was assigned for the proton of (N=CH), and the signal at 8.86 ppm was resonated to the protons of (N–CH) ring. Peak at 4.98-4.82 ppm belongs to the protons of (CH_2O) group. The signal at 8.39 ppm was attributed to the proton of O-H. Peak at 2.35ppm is for protons of CH_3 group[6]. See table (3).

Table (3): ^{1}H-NMR data for [H_2L^2]

Compound	Functional group	δ (ppm)
H_2L^2	N–CH	8.86
	N=CH	8.19
	OH	8.39
	Ar–CH	7.22–6.79
	O-CH_2	4.96 and 4.88
	CH_3	2.35
	HDO	3.62
	DMSO	2.32

2.5. ^{13}C-NMR spectrum for H_2L^2:

^{13}C-NMR spectrum of (H_2L^2) shows peaks at 113.51-140.47 ppm assigned for aromatic carbon atoms, while the peak at 158.23 ppm attributed to carbon of imine group (C_7)[14]. The peak at 197.52 ppm attributed to the (C_8), while carbon (C_9) of (C–O–H) appeared at 172.28 ppm. The chemical shifts at 176.10 ppm is for (C_{10}) of (C-CH_3), whereas peak of carbon C_{11} of aromatic C-N was at 158.55 ppm. The chemical shift at 65.90 ppm attributed to the carbon C_{13} of (CH_2 –OH), and shift at 13.76ppm attributed to the (C_{14}) of (CH_3) group [6]. See table (4).

Table (4): ^{13}C-NMR data of [H_2L^2]

Compound	Functional group	δ (ppm)
H_2L^2	C8	197.52
	C10	176.10
	C7	158.23
	C1 – C6	113.51-140.47
	DMSO	40.41 – 39.40
	C14	13.76

2.6. Electronic spectrum of (H_2L^2) ligand:

The electronic spectrum for (H_2L^2) exhibited 4 absorption peaks at (276nm,36232 cm^{-1}) with (312nm, 32051 cm^{-1}) assigned to ($\pi \rightarrow \pi^*$) transition and (368nm , 27174 cm^{-1}) and (463nm , 21598 cm^{-1}) is due to ($n \rightarrow \pi^*$) and (LLCT) transition [16]. The data of absorption of the ligand (H_2L^2) were arranged in the table (5).

Table (5): Electronic data of the ligand

Ligand	λ (nm)	υ– (cm^{-1})	ε_{max} (molar $^{-1}cm^{-1}$)	transitions
H_2L^2	276	36232	412	л → л*
	312	32051	362	л → л*
	368	27174	358	n→ л*
	463	21598	726	LLCT

2.7. Preparation of (H_2L^2)complexes(1-7):

2.7.1. Synthesis of $K_2[VO(L^2)(OSO_3)].H_2O$ (1)

An ethanolic solution of [H_2L^2] (0.03g, 1mmole). A solution of KOH (1 g/mmole) was formed, and then was added drop by drop to a Vanadyl (II) sulphate monohydrate (0.0181g, 1mmole) dissolved in (10ml) ethanol. After letting the reaction mixture reflux for (3 hrs.). The dark brown product was obtained, washed several times with EtOH and dried to give the complex in 91% yield, M.P : (260-262ºC).

2.7.2. Synthesis of $K_2[Mn(L^2)_2].H_2O$ (2), $K_2[Fe(L^2)_2].H_2O$ (3), $K_2[Co(L^2)_2].H_2O$(4),$K_2[Ni(L^2)_2].H_2O$ (5) , $K_2[Cu(L^2)_2].H_2O$ (6) , and $[Pt(L^2)_2].2H_2O$ (7).

Using the mentioned method in the synthesis of VO(II) complex, was used to synthesize the complexes of [H_2L^2] with H_2PtCl_6 , $MCl_2.nH_2O$ M(II)=[Mn (n=4), Co (n=6), Ni (n=6), Cu (n=2), Fe (n=4), and Pt (n=0)] ions. For the physical properties see table (6).

Table(6): physical properties of ligand [H_2L^2] complexes

No.	Formula	Color	Molecular formula of mineral salt	Wt of metal salt (1mmol.)
1	$K_2[VO(L^2)(OSO_3)].H_2O$	Dark brown	$VOSO_4.H_2O$	0.018 g
2	$K_2 [Mn(L^2)_2].H_2O$	Dark brown	$MnCl_2.4H_2O$	0.020 g
3	$K_2 [Fe(L^2)_2].H_2O$	Reddish brown	$FeCl_2.4H_2O$	0.020 g
4	$K_2 [Co(L^2)_2].H_2O$	reddish brown	$CoCl_2.6H_2O$	0.024 g
5	$K_2 [Ni(L^2)_2].H_2O$	Reddish brown	$NiCl_2.6H_2O$	0.0238 g
6	$K_2 [Cu(L^2)_2].H_2O$	Dark brown	$CuCl_2.2H_2O$	0.0171 g
7	$[Pt(L^2)_2].2H_2O$	brown	H_2PtCl_6	0.040g

3. Results and discussion:

Some of the physical characteristics of novel ligand and its complexes are tabulated in table (7). The results from the elemental analysis were listed with the mathematical calculations.

Table (7): Molecular weights of the ligand (H_2L^2)complexes(1-7) and the results of elemental microanalysis.

Complexes.No	Compounds	M.wt g/mol	Found / calc. %					
			C	H	N	S	metal	K
1	$K_2[VO(C_{14}H_{11}N_3O_5)(OSO_3)].H_2O$	560	29.71	2.29	7.39	5.60	8.99	13.82
			30.00	2.32	7.50	5.71	9.10	13.92
2	$K_2 [Mn(C_{14}H_{11}N_3O_5)_2].H_2O$	753	44.49	3.16	10.92		7.19	10.28
			44.62	3.18	11.15	-	7.30	10.35
3	$K_2 [Fe(C_{14}H_{11}N_3O_5)_2].H_2O$	754	44.39	3.16	10.96		7.29	10.24
			44.56	3.18	11.14	-	7.40	10.30
4	$K_2 [Co(C_{14}H_{11}N_3O_5)_2].H_2O$	757	43.98	3.11	10.96		7.62	10.22
			44.38	3.17	11.09	-	7.79	10.31
5	$K_2 [Ni(C_{14}H_{11}N_3O_5)_2].H_2O$	756.7	43.96	3.11	10.97		7.59	10.19
			44.40	3.16	11.10	-	7.74	10.30
6	$K_2 [Cu(C_{14}H_{11}N_3O_5)_2].H_2O$	761.5	43.89	3.10	10.92		8.21	10.11
			44.12	3.15	11.03	-	8.33	10.24
7	$[Pt(C_{14}H_{11}N_3O_5)_2].2H_2O$	833	40.22	3.08	9.96		22.96	-
			40.33	3.12	10.08	-	23.40	

Calc.= Calculated

3.1. Molar conductance and the physical properties of the ligand H_2L^2 complexes (1-7):

Table (8): The molar conductivity values and physical properties of H_2L^2 ligand Complexes(8-14)

Complexes No.	Complexes	Yield %	M.p. ºC	m.c s.cm^2 /mol	Ratio ionic
1	$K_2[VO(L^2)(OSO_3)].H_2O$	91	>250	73.06	2:1
2	$K_2 [Mn(L^2)_2].H_2O$	88	180 Dec	74.31	2:1
3	$K_2 [Fe(L^2)_2].H_2O$	82	283-240	79.16	2:1
4	$K_2 [Co(L^2)_2].H_2O$	89	162-164	78.04	2:1
5	$K_2 [Ni(L^2)_2].H_2O$	85	>250	75.21	2:1
6	$K_2 [Cu(L^2)_2].H_2O$	88	158-160	75.42	2:1
7	$[Pt(L^2)_2].2H_2O$	79	240 Dec	18.46	neutral

3.2. Magnetic susceptibility of ligand's H_2L^2 complexes :

The effective magnetic moments (μeff B.M) of the metal complexes were measured in the solid state using Faraday's method[16] . Pt(IV) complex is diamagnetic in nature, because of $5d^6$, suggesting low spin octahedral geometry[17].

Table (9): The effective magnetic moment (μeff) values for complexes (1-7)

Complexes No.	COMPLEXES	Xg x 10^{-6}	Xm x 10^{-6}	X_A x 10^{-6}	No.of unpaired Electron	μeff B.M	structure
1	$K_2[VO(L^2)(OSO_3)].H_2O$	1.820	1019.200	1247.88	1	1.73	Sq.Py
2	$K_2[Mn(L^2)_2].H_2O$	15.960	12017.880	12439.49	5	5.46	Oh.
3	$K_2[Fe(L^2)_2].H_2O$	0.00	0.00	0.00	0	0.00	LS oh
4	$K_2[Co(L^2)_2].H_2O$	12.342	9342.894	9764.50	3	4.84	Oh.
5	$K_2[Ni(L^2)_2].H_2O$	3.648	2760.441	3182.05	2	2.76	Oh.
6	$K_2[Cu(L^2)_2].H_2O$	1.190	906.185	1327.79	1	1.78	Oh.

D= - 421.61 ^{x} 10^{-6}, Sq. Py = square pyramid, LS = low spin

3.3. FT-IR spectra of ligand's [H_2L^2] complexes (1-7):

The infra-red spectra for the synthesized compounds 1-7 are listed in table (10). Which shows that some guide bands in spectra for ligand H_2L^2 are changed of their position or shape on coordination with metal ion. The infra-red spectra of the prepared complexes were compared to of H_2L^2 this was to determine when ligands were involved in the chelation step [18]. The band of the stretch frequency of the azomethine C=N group of free ligand was appeared at 1620 cm^{-1}, but for the obtained complexes the same band was shifted either lower or higher frequencies in the range of 1614-1627 cm^{-1}, and this shift might have related to the coordination of the metal ions to the nitrogen atom of the azomethine group. The stretch vibration band at 1581 cm^{-1} is belong to C=N group of thiazole ring of free ligand, and was shifted to range of 1539-1585 cm^{-1} for all complexes, confirming the coordination between metal ions and nitrogen atoms C=N group [19]. The bands at 1249-1265 cm^{-1} and at 744-756 cm^{-1} of complexes 1-7, were attributed to both C-O group of phenolic compounds, which were shifted to a lower or higher frequencies on comparison to the free ligand (H_2L^2) at 1288 and 744 cm^{-1}. This shift is due to the coordination of the phenolic oxygen atom to metal ion [20]. The broad band in infra-red spectra for the complexes 8-14 were assigned to hydrate H_2O [21]. For the complex of VO (II) the new band was appeared at 999 cm^{-1} and attributed to the V=O vibration [22]. Other new bands for the of infra-red spectrum of complex VO(II) were at 1045, 981 and 663 cm^{-1} are corresponding to SO_4^{-2} group, and this indicating that the SO_4^{-2} is participated in the coordination to the VO(II) ion which behave as monodentate ligand. In the out of plane region, the infra-red spectra displayed additional bands they were absent in the

spectra of the free ligand. These bands are located between 594 and 516 cm^{-1} and assigned to (M-N) bond. In contrast, the bands located between 478 and 428 cm^{-1} are designated as (M-O) [23].

Table (10):FT-IR data (cm^{-1}) of the ligand [H_2L^2] and complexes.

No. complexes	Compounds	O-H	C-O	C=N imine	C=N in plane	M - N	M - O
#	H_2L^2	3356	1288 744	1620	1581	-	-
1	$K_2[VO(L^2)(OSO_3)].H_2O$	3421	1261 732	1616	1577	582	438
2	K_2 $[Mn(L^2)_2].H_2O$	3332	1292 736	1627	1576	551	478
3	K_2 $[Fe(L^2)_2].H_2O$	3471	1284 740	1616	1593	532	428
4	K_2 $[Co(L^2)_2].H_2O$	3417	1292 748	1615	1585	516	447
5	K_2 $[Ni(L^2)_2].H_2O$	3441	1275 732	1616	1577	594	478
6	K_2 $[Cu(L^2)_2].H_2O$	3417	1276 732	1614	1574	520	442
7	$[Pt(L^2)_2].2H_2O$	3329	1241 748	1631	1558	555	448

3.4. Electronic spectrum of (H_2L^2) ligand complexes (1-7):

The electronic data for complexes 1-7 are listed in table (11) along with electronic transition and proposed geometrical shapes. The spectra for the complexes 1-7 displayed 3 to 5 signals at a range 266-448nm, (37594-22321cm^{-1}) and were attributed to intra-ligand, which shows shifting to lower and higher wave length on comparing to the (H_2L^2) free ligand. Such shifting confirmed the coordination of (H_2L^2) ligand to the central ion [24]. In addition, the spectra of complexes1-7 displayed a new intense absorption within the range of 402-463nm. Moreover, peaks at 24876-21589 cm^{-1} were assigned to M→LCT electronic transition [25].

Table (11): Electronic spectral data for $[H_2L^2]$and its complexes.

Complexes No.	Compound	λ (nm)	υ–(cm^{-1})	ε_{max} molar $^{-1}$ /cm	Electronic transitions	proposed Structure
#	H_2L^2	276	36232	412	л → л*	-
		312	32051	362	л → л*	
		368	27174	358	n→ л*	
		463	21598	726	LLCT	
1	$K_2[VO(L^2)(OSO_3)].H_2O$	270	37037	905	Intra-ligand	Sq.py.
		306	32680	843	Intra-ligand	
		365	27397	1145	Intra-ligand	
		381	26247	852	Intra-ligand	
		445	22472	782	MLCT	
		548	18248	108	$^2B_2 \rightarrow {}^2B_1$	
		706	14164	19	$^2B_2 \rightarrow {}^2E$	
2	$K_2 [Mn(L^2)_2].H_2O$	271	36900	1644	Intra-ligand	Oh.
		307	32573	1543	Intra-ligand	
		315	31746	1522	Intra-ligand	
		345	28986	1873	Intra-ligand	
		404	24752	1475	Intra-ligand	
		420	23810	1497	MLCT	
		518	19305	412	$^6A_1g \rightarrow {}^4T_2g$ (G)	
		578	17301	108	$^6A_1g \rightarrow {}^4T_1g$ (G)	
3	$K_2 [Fe(L^2)_2].H_2O$	279	35842	787	Intra-ligand	L.S.Oh.
		310	32258	648	Intra-ligand	
		346	28902	685	Intra-ligand	
		452	22124	1347	MLCT	
		636	15723	18	$^1A_1g \rightarrow {}^1T_2g$	
		833	12005	10	$^1A_1g \rightarrow {}^1T_1g$	
		1070	9346	14	$^1A_1g \rightarrow {}^3T_2g$	
4	$K_2 [Co(L^2)_2].H_2O$	268	37313	878	Intra-ligand	Oh.
		310	32258	526	Intra-ligand	
		344	29070	586	Intra-ligand	
		402	24876	640	MLCT	
		540	18519	72	$^4T_1g(F) \rightarrow {}^4T_1g$ (P)	
		760	13158	44	$^4T_1g(F) \rightarrow {}^4A_2g(F)$	
		894	11186	43	$^4T_1g(F) \rightarrow {}^4T_2g(F)$	
5	$K_2 [Ni(L^2)_2].H_2O$	266	37594	917	Intra-ligand	Oh.
		308	32468	648	Intra-ligand	
		345	28986	904	Intra-ligand	
		406	24631	843	Intra-ligand	
		463	21598	1015	MLCT+ $^3A_2g(F \rightarrow {}^3T_1g(P)$	
		622	16077	41	$^3A_2g(F) \rightarrow {}^3T_1g(F)$	

		961	10406	20	$^3A_2g(F) \rightarrow {}^3T_2g$ (F)	
6	K_2 [Cu(L^2)$_2$].H_2O	270	37037	1293	Intra-ligand	Dist.Oh
		310	32258	1282	Intra-ligand	
		345	28986	1642	Intra-ligand	
		388	25773	1153	Intra-ligand	
		421	23753	1260	MLCT	
		534	18727	108	$^2B_1g \rightarrow {}^2B_2g$	
		734	13624	60	$^2B_1g \rightarrow {}^2A_1g$	
7	[Pt(L^2)$_2$].2H_2O	271	36900	1912	Intra-ligand	Oh.
		312	32051	994	Intra-ligand	
		350	28571	993	Intra-ligand	
		359	27855	634	Intra-ligand	
		425	23529	504	MLCT	
		643	15552	32	$^1A_1g \rightarrow {}^1T_2g$	
		833	12005	28	$^1A_1g \rightarrow {}^1T_1g$	

3.5. Thermal analysis :

In Table(12) the thermal decomposition data of metal complex [Co(L^2)$_2$]. H_2O are listed, figure (S2) showed curves discuss. In this work, the title compound is studied using a variety methods for analysis, such as Thermo-Gravimetric Analysis (TGA) and Differential Scanning Calorimetry (DSC).

Table (12): TG and DSC data for [Co(L^2)$_2$].H_2O complex.

Complex	**Stage**	**Decomposition Temperatures (ºC)**	**Estimated (calculated)**		**Assignment**
			Mass Loss	**Total mass Loss**	
[Co(L^2)$_2$].H_2O	1	217	0.313	4.973 (5.281)	- (H_2O, CO, H_2)
			(0.353)		
	2	304	1.846		- (N_2, C_4H_6O, $2CO_2$, NH_3, C_6H_5, H_2)
			(1.926)		
	3	619	0.738		- ($C_5H_4O_3$)
			(0.801)		
	4	above 619	2.076		- ($K_2CoC_{10}N_3O$)

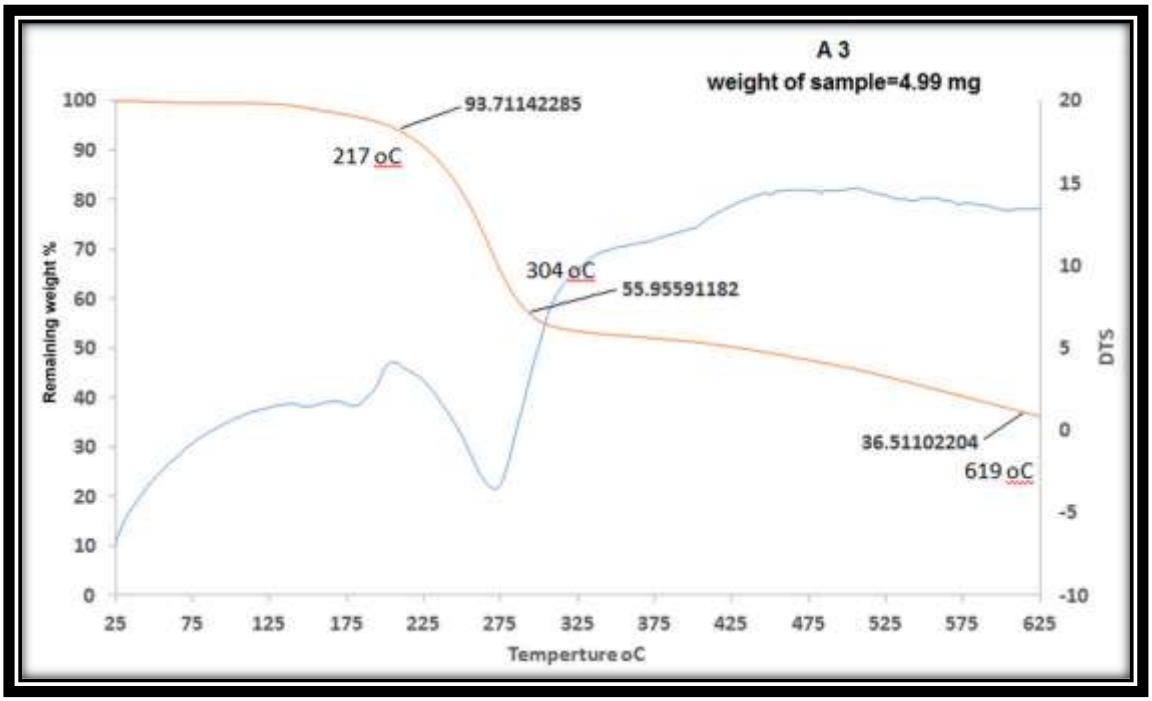

Figure (S2): TGA and DSC thermos-gram of $[Co(L^2)_2].H_2O$

3.6. Anti-bacterial Activity:

The biological activities of novel ligand H_2L^2 and the obtained complexes have evaluated against gram-positive and gram-negative bacterial strains and some fungi species.

The antibacterial activity for the synthesized compounds was tested against four types of bacteria (*Klebsiella pneumonia, pseudomonas, Staphylococcus aureus* and *Bacillus subtilis*), and the results of the tests are listed in table (13). Figure (S3) to Figure (S6) illustrates the inhibition area for the synthesised compounds on dishes, and shows that it have different antibacterial activities [26].

3.7. Anti-fungal Activity:

The anti-fungal activity for the obtained compounds were tested against *Candida albicans*. The results of tests are listed in the table (13) and shows a good effect. Figure (S8)[27].

Table (13): The biological activity of desired compounds

Compound	***K.pneumoniae***	***Pseudomonas***	***B. subtilis***	***St. aureus***	***Candida albicans***
H_2L^2	15	22	11	16	13
$K_2[VO(L^2)(OSO_3)].H_2O$	20	19	26	18	13
$K_2[Mn(L^2)_2].H_2O$	7	18	16	9	15
$K_2[Fe(L^2)_2].H_2O$	7	22	13	10	20
$K_2[Co(L^2)_2].H_2O$	20	18	17	20	15
$K_2[Ni(L^2)_2].H_2O$	27	17	26	16	13
$K_2[Cu(L^2)_2].H_2O$	7	20	14	9	15
$[Pt(L^2)_2].2H_2O$	6	21	18	9	16
DMSO	0	0	0	0	0
Fluconazole	-	-	-	-	22
Ceftriaxone	15	12	13	13	-

Figure(S3): Effect of (H_2L^2) and it's complexes against (*Bacillus subtilus*)

Figure (S4): Effect of (H_2L^2) and it's complexes against (*Staphylococcus aureus*)

Figure (S5): Effect of (H_2L^2) and it's complexes against (*Klebsiella pneumoniae*)

Figure (S6): Effect of (H_2L^2) and it's complexes against (*Pseudomonas aeruginosa*)

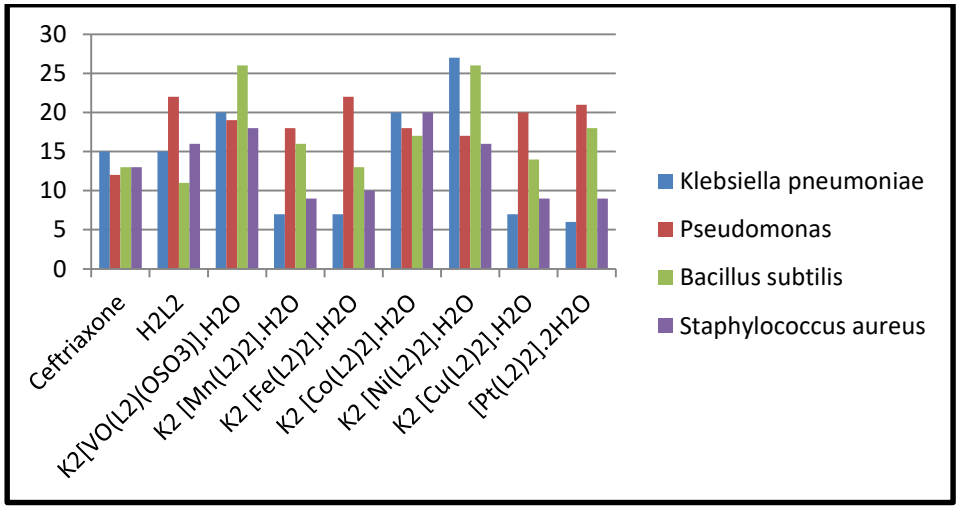

Figure (S7): Anti-bacterial activities against four types of bacteria

Figure (S8): Effect of (H_2L^2) and it's complexes against (*Candida albicans*)

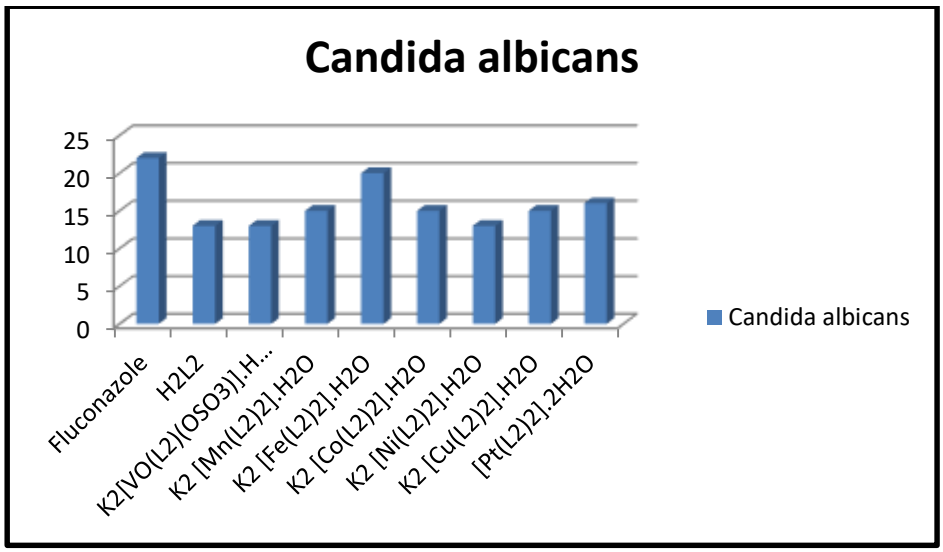

Figure (S9): Anti-fungal activities of against *candida albicans*

4. Conclusions:

According to the characterized data of novel Schiff base ligand H_2L^2 (4-((2-hydroxy-5-nitrophenyl)imino)methyl)-5(hydroxymethyl)-2-methylpyridin-3-ol), which resulted by the reaction of 2-amino-4-nitrophenol with pyridoxal hydrochloride and their derived complexes. After diagnosing there with all the spectroscopic methods and devices mentioned in this study, the results shows that the ligand (H_2L^2) behave as a tridentate ligand *via* nitrogen atom in imine group and oxygen atom in member ring with central metal ions: [VO(II), Mn(II), Fe(II), Co(II), Ni(II), Cu(II) and Pt(IV)] with general formula $K_2[M(L^2)_2].XH_2O$ and $K_2[VO(L^2)(OSO_3)].H_2O$. The anti-bacterial and anti-fungal activities of the compounds gave excellent results.

References

1. Farshbaf, S.; Sreerama, L.; Khodayari, T.; Vessally, E. Propargylic ureas as powerful and versatile building blocks in the synthesis of various key medicinal heterocyclic compounds. *Chemical Review and Letters*, **2018**. ,*1(2)*,5667.doi10.22034/crl.2018.85120
2. Siddiquee, S., *Recent advancements on the role and analysis of volatile compounds (VOCs) from Trichoderma*, in *Biotechnology and biology of trichoderma*. **2014**, Elsevier. 139-175. https://doi.org/10.1016/b978-0-444-59576-8.00011-4
3. Rajasekar, K., T. Ramachandramoorthy, and S. Balasubramaniyan, *Synthesis, spectral characterization and biological activities of Cr (III), Co (II), Ni (II) and Zn (II) complexes with 4-aminoantipyrine and azide ion as ligands.* Chem. Sci. Trans., **2013**. *2(3),* 877-882. doi:10.7598/cst2013.487
4. Bushra Karim Hamad*, M.R.A., *Synthesis of new compounds with seven rings (oxazepine) through the ring closure of Schiff bases with study of biological activity*. Eurasian Chemical Communications, **2022**. *4(12):* 1306-1317. 10.22034/ecc.2022.332079.1343
5. Hadi, M.A.; M.S. Mohammed; Kadhium, A.J., *Synthesis, characterization and spectral studies and Biological screening study of Transition Metal complexes with new Heterocyclic Ligand*

Derived from pyridoxal Hydrochloride. Systematic Reviews in Pharmacy, **2021**. ***12(1)***: 371-383. doi:10.31838/srp.2021.1.58

6. Mukhtorov, L.; Georgy Pestsov; Maria Nikishina; Evgenia Ivanova; Yury Atroshchenko; Leonid Perelomov, *Fungicidal Properties of 2-Amino-4-nitrophenol and Its Derivatives.* Bulletin of environmental contamination and toxicology, **2019**. *102(6):* p. 880-886. https://doi.org/10.1007/s00128-019-02602-4

7. Radecka-Paryzek, W.; Patroniak, V.; Lisowski , J., *Metal complexes of polyaza and polyoxaaza Schiff base macrocycles.* Coordination Chemistry Reviews, **2005**. *249(21-22):* 2156-2175. https://doi.org/10.1016/j.ccr.2005.02.021

8. Anand, T., A.S. Kumar, and S.K. Sahoo, *A novel Schiff base derivative of pyridoxal for the optical sensing of Zn2+ and cysteine.* Photochemical & *Photobiological Sciences*, **2018**. *17(4):* 414-422. https://doi.org/10.1039/c7pp00391a

9. Mandal, S.; Sikdar, Y.; Sanyal, R.; Goswami, S.,. Experimental and theoretical study on a new copper (II) complex derived from pyridoxal hydrochloride and 1, 2-diaminocyclohexane. *Journal of Molecular Structure*, **2017**,*1128*,471-480. https://doi.org/10.1016/j.molstruc.2016.09.011

10. Suku, S. ; Ravindran, R.,. Synthesis, characterization and antimicrobial studies of 1d hetero-bimetallic coordination polymers of pyridine-2, 6-dicarboxylic acid with iron and alkaline earth metals. *Journal of MolecularStructure*, 2022,*1252*,132083. https://doi.org/10.1016/j.molstruc.2021.132083

11. Al-Talib, M.; Al-Soud, Y.A.; Abussaud, M.; Khshashneh, S.,. Synthesis and biological evaluation of new benzothiazoles as antimicrobial agents. *Arabian Journal of chemistry*, **2016**, *9*, pp.S926-S930. https://doi.org/10.1016/j.arabjc.2011.09.003

12. Azzam, R.A.; Elgemeie, G.H.; Elsayed, R.E.; Gad, N.M.; Jones, P.G.,. Crystal structure of 2-(benzo [d] thiazol-2-yl)-3, 3-bis (ethylsulfanyl) acrylonitrile. *Acta Crystallographica Section E: Crystallographic Communications*, **2022,***78*(4). https://doi.org/10.1107/S2056989022002572

13. Blasco, R.; Castillo, F., *Light-dependent degradation of nitrophenols by the phototrophic bacterium Rhodobacter capsulatus E1F1.* Applied and environmental microbiology, **1992**. *58(2):* p. 690-695. https://doi.org/10.1128/aem.58.2.690-695.1992

14. Suryanti, V.; Wibowo, F.R.; Isnaeni, S.R.; Sari, M.R.K.; Handayani, S.,. Addition reaction of methyl cinnamate with 2-amino-4-nitrophenol. In *IOP Conference Series: Materials Science and Engineering* **2016,** *107, No. 1*, 012062.doi:10.1088/1757-899X/107/1/012062

15. Patil, A.R.; Donde, K.J.; Raut, S.S.; Patil, V.R.; Lokhande, R.S.,. Synthesis, characterization and biological activity of mixed ligand Co (II) complexes of schiff base 2-amino-4-nitrophenol-n-salicylidene with some amino acids. *Journal of Chemical and Pharmaceutical Research*, **2012**,*4*(2),1413-1425.https://www.semanticscholar.org/paper/Synthesis-%2C-characterization-and-biological-of-Co-(-Patil-Donde/e2d4f047f9a14f8c09d83fb9ca992116b0774193

16. Cotton, F.A.; Wilkinson, G.; Murillo, C.A.; Bochmann, M., *Advanced inorganic chemistry*. John Wiley and Sons, Inc. **1999**, http://repository.vnu.edu.vn/handle/VNU_123/85212.

17. Anupama, B.; Padmaja, M.; Kumari, C.G.,. Synthesis, characterization, biological activity and DNA binding studies of metal complexes with 4-aminoantipyrine Schiff base ligand. *E-Journal of Chemistry*, **2012**,*9(1)*,389-400. https://scholar.google.com/citations?view_op=view_citation&hl=en&user=31Zn0B4AAAAJ&citation_for_view=31Zn0B4AAAAJ:zYLM7Y9cAGgC

18. Abbas, G.; Irfan, A.; Ahmed, I.; Al-Zeidaneen, F.K.; Muthu, S.; Fuhr, O.; Thomas, R.,. Synthesis and investigation of anti-COVID19 ability of ferrocene Schiff base derivatives by quantum chemical and molecular docking. *Journal of molecular structure*, **2022,***1253*,.132242. https://doi.org/10.1016/j.molstruc.2021.132242

19. Maher, K.A.; Mohammed, S.R., Metal complexes of Schiff base derived from salicylaldehyde-A review. *International Journal of Current Research and Review*, **2015,***7*(2),6. https://ijcrr.com/article_html.php?did=647

20. Ommenya, F.K.; Nyawade, E.A.; Andala, D.M.; Kinyua, J., 2020. Synthesis, characterization and antibacterial activity of Schiff base, 4-Chloro-2-{(E)-[(4-fluorophenyl) imino] methyl} phenol metal (II) complexes. *Journal of Chemistry*, **2020**. https://doi.org/10.1155/2020/1745236

21. Diab, M.A.; Mohamed, G.G.; Mahmoud, W.H.; El-Sonbati, A.Z.; Morgan, S.M.; Abbas, S.Y.,. Inner metal complexes of tetradentate Schiff base: Synthesis, characterization, biological activity and molecular docking studies. *Applied Organometallic Chemistry*, **2019**,*33*(7), e4945. https://doi.org/10.1002/aoc.4945

22. Raman, N.; Dhaveethu Raja, J.; Sakthivel, A., Synthesis, spectral characterization of Schiff base transition metal complexes: DNA cleavage and antimicrobial activity studies. *Journal of Chemical sciences*, **2007,***119*(4),303-310. https://link.springer.com/article/10.1007/s12039-007-0041-5

23. Lateef, S.M.; Sarhan, B.M.; Al-Saedi, W.A., Synthesis, Characterization and Biological Activity for Complexes VO (II), Mn (II), Co (II) and Ni (II) with new multidentate ligand [2-((E)-3-(2-hydroxyphenylimino)-1, 5-dimethyl-2-phenyl-2, 3-dihydro-1H-pyrazol-4-ylimino) acetic acid][H2L] type (N2). *Diyala Journal For Pure Science*, **2016**,*12*(1).https://scholar.google.com/citations?view_op=view_citation&hl=en&user=n8UrjGAAAAAJ&citation_for_view=n8UrjGAAAAAJ:d1gkVwhDpl0C

24. Cowley, A.R.; Dilworth, J.R.; Donnelly, P.S.; White, J.M., Copper complexes of thiosemicarbazone− pyridylhydrazine (THYNIC) hybrid ligands: a new versatile potential bifunctional chelator for copper radiopharmaceuticals. *Inorganic chemistry*, **2006,** *45*(2),496-498. https://doi.org/10.1021/ic0514492

25. Osowole, A.A.; Ekennia, A.C.; Achugbu, B.O.; Etuk, G.H.,. Synthesis, spectroscopic characterization and structure related antibacterial activities of some metal (II) complexes of substituted triflurobutenol. *Elixir Appl Chem*, **2013**, *59*,15848-15852. https://www.rroij.com/open-access/synthesis-spectroscopic-characterization-and-antibacterial-properties-of-some-metal-ii-complexes-of-26methoxybenzothiazol2-ylimino-.php?aid=34639

26. Hassan, S.A., Lateef, S.M. and Majeed, I.Y.,. Structural, Spectral and Thermal studies of new bidentate Schiff base ligand type (NO) derived from Mebendazol and 4-Aminoantipyrine and it's metal complexes and evaluation of their biological activity. *Research Journal of Pharmacy and Technology*, **2020,***13*(6),3001-3006. DOI: 10.5958/0974-360X.2020.00531.4

27. Kuate, M.; Conde, M.A.; Ngandung Mainsah, E.; Paboudam, A.G.; Tchieno, F.M.M.; Ketchemen, K.I.; Tonle Kenfack, I.; Ndifon, P.T., 2020. Synthesis, Characterization, Cyclic Voltammetry, and Biological Studies of Co (II), Ni (II), and Cu (II) Complexes of a Tridentate Schiff Base, 1-((E)-(2-Mercaptophenylimino) Methyl) Naphthalen-2-ol (H2L1). *Journal of Chemistry*, **2020**. https://doi.org/10.1155/2020/5238501